Analysis & Optimization of Scramjet Inlet using Computational Fluid Dynamics

Mr. A. A. Kesskar[1] Prof. K. D. Sarode[2] Mr. M. G. Patwardhan[3] Mr. P. V. Patankar[4] Mr. S. V. Bapat[5]
[1]Founder & CEO [2]Research Advisor [3,4,5]Trainee
[1,2,3,4,5]A Square Innovation, Research & Training, India

Abstract— Scramjets are air breathing engines with no moving parts. They rely on the 'ram-air' effect. This is done with the help of oblique shockwaves. The inlet geometry is used to slow down hypersonic air to supersonic speeds to achieve compression, which is then used to burn fuel and accelerated through a diverging section to achieve thrust. The main challenge in making scramjets viable is the lower Mach threshold of its operating range, which is quite high i.e. Mach 3-4. This paper aims at using optimization techniques in CFD (CFX) to reduce the lower threshold of the operating range of the scramjet to between Mach 2.5 to 3. This is mainly achieved by manipulating the inlet geometry. This is done by simulation of flight in a Mach range with available experimental data, validation of the simulation methodology, and application to a lower Mach domain. Optimization techniques were used to generate geometric parameters which provided positive results in lower Mach ranges.

Key words: Scramjet, Inlet, Starting Mach Number, CFD, CFX, Optimization, Oblique Shocks, Wedge Angles

I. INTRODUCTION

Jet engines are reaction engines powered by the discharge of a high velocity jet stream. This jet stream generates thrust based on the principles of jet propulsion. Jet engines are generally divided into two main categories, namely Non-air breathing and Air breathing. Engines that acquire oxygen required for combustion of fuel from the atmosphere are known as air breathing engines. Most commonly used air breathing engines in recent times are turbo engines. Turbo engines consist of moving parts that compress the incoming air to a required pressure and the compressed air is then sent to the combustion chamber and the combustion produces the thrust that propels the aircraft. Turbo engines cannot be effectively utilized for speeds greater than the speed of sound. Thus, for supersonic applications, different types of air breathing engines are utilized. These engines are known as Ram powered jet engines.

Ram powered engines employ no moving parts. At supersonic speeds, the incoming is directed into the engine. By guiding the incoming air into a convergent section, the velocity of the incoming air is reduced to subsonic speeds and the pressure is subsequently increased. The pressure of incoming air thus obtained is found to be of the required order to support effective combustion of fuels. A nozzle accelerates the exhaust to supersonic speeds, resulting in thrust. As a result, air compressors need not be employed to increase pressure of incoming air. This simplifies the construction and reduces the overall weight of the engine. Due to the deceleration of the freestream air, the pressure, temperature and density of the flow entering the burner are considerably higher than in the freestream. Thus, conceptually, Ramjet engines need to attain subsonic flight and the incoming air has to possess a sufficiently high velocity to function efficiently. The can function effectively up to freestream velocity of incoming air of the order of Mach 6. If the speed of the incoming air exceeds Mach 6, the inlet geometry can no more reduce the velocity of air in the throat section of the engine to subsonic levels as required for the smooth operation of the Ramjet engine. As a result, a newer type of engine was developed which can operate successfully without having to reduce the Mach number of freestream air to subsonic speeds in the throat section of the engine.

This engine is an evolution of the Ramjet engine wherein the velocity of the incoming air is not required to be reduced to subsonic levels for effective operation. It is a Supersonic Combustion Ramjet engine or simply, Scramjet engine.

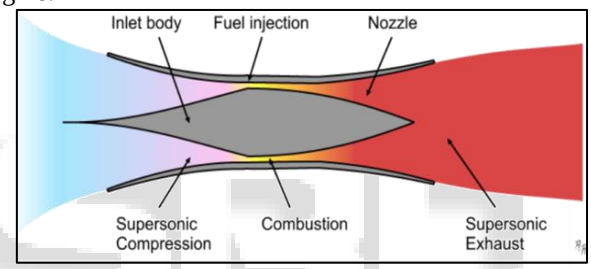

Fig. 1: Functional Diagram of a Scramjet

Parts involved in scramjet engines are fuel injectors, combustion chamber, thrust nozzle and inlet section which is responsible for compressing the air to the required pressure. An isolator between the inlet and combustion chamber is often included to improve the homogeneity of the flow in the combustor and to extend the operating range of the engine. The aim behind the designing principle of a scramjet engine is minimizing drag and maximizing thrust to attain maximum possible efficiency.

II. LITERATURE SURVEY

'Turbulent Shock Wave Boundary-Layer Interaction' authored by J. Delery and J.G. Marvin, AGARD-AG-280 ref. ISBN 92-835-1519-6 (February 1986) presents a comprehensive review of the shock-wave boundary- layer interaction problem. A detailed physical description of the phenomena for transonic and supersonic speed regimes is given based on experimental observations, correlations, and theoretical concepts. Approaches for solving the problem are then reviewed in depth. Specifically, these include: global methods developed to predict sudden changes in boundary-layer properties; integral or finite-difference methods developed to predict the continuous evolution of a boundary-layer encountering a pressure field induced by a shock wave; coupling methods to predict entire flow fields; analytical methods such as multi-deck techniques; and finite-difference methods for solving the time-dependent Reynolds-averaged Navier-Stokes equations used to predict the development of

entire flow fields. Examples are presented to illustrate the status of the various methods and some discussion is devoted to delineating their advantages and shortcomings. This paper offers insight into the propagation of shockwaves and the boundary layer interaction, a detailed understanding of which is highly essential for designing the inlet geometry of a scramjet engine.

The paper offers deep insights into the characteristics and propagation of shockwaves. It also describes boundary layer separation and modes of calculation for both the phenomena. Understanding these phenomena is extremely crucial in understanding and predicting the characteristics of supersonic flow.

A. Impinging Shockwaves

For a purely inviscid flow the uniform upstream flow processed by the incoming shock wave is uniformly turned towards the surface and then straightened again by the reflected shock. Analytic expressions are available to predict this rather simple situation. The presence of a boundary layer confounds the problem, and the resulting flow-field characteristics depend on the strength of the incoming shock wave.

In the weak interaction, the shock wave penetrates the turbulent boundary layer and turns more steeply toward the surface as it encounters the lower speeds within the viscous layer.

It reflects from the viscous layer through a series of compression waves that coalesce into a reflected shock wave. A uniformly increasing surface-pressure signature is found, whose overall rise is nearly equivalent to the inviscid jump. In the strong interaction, the shock wave also penetrates the viscous layer, but that layer cannot overcome the pressure rise, and separation takes place. The viscous layer is turned above the separation through a series of compression waves that coalesce into what is called a separation shock which is later weakened by expansion waves emanating from the viscous flow accelerating over the separation bubble. Downstream, where the bubble terminates, a series of compression waves coalesce into a reflected shock where the flow aligns itself with the surface. The corresponding surface pressure is characterized by a smooth pressure rise and an inflection region characteristic of separation.

"Analysis And Design Of A Hypersonic Scramjet Engine With A Starting Mach Number Of 4.00" authored by Kristen Nicole Roberts, The University of Texas at Arlington (2008) highlights that when pressures and temperatures become so high in supersonic flight that it is no longer efficient to slow the oncoming flow to subsonic speeds for combustion, a scramjet (supersonic combustion ramjet) is used in place of a ramjet. Currently, the transition to supersonic combustion generally occurs at a freestream Mach number around 5.0 to 6.0. This research details analysis completed towards extending scramjet operability to lower Mach numbers, while maintaining performance at higher Mach numbers within the same flow path.

"Performance Analysis of Scramjet Inlet" authored by L.Hariramakrishnan, K.Nehru, T.Sangeetha provides a computational analysis of a complete scramjet demonstrator model. The computational results will take place under real flight conditions at a hypersonic speed. Prior to these tests, a numerical analysis of the performance of the demonstrator geometry is conducted. It is shown that the intake is able to generate flow conditions required for stable supersonic combustion using a central strut injector. The methodology involved with solving flow problems using the CFD software. ANSYS CFX is an integrated software system capable of solving diverse and complex multidimensional fluid flow and heat transfer problems. The software solves three dimensional Naiver Stokes equations in a fully implicit manner. It is a finite volume method solver. It utilizes numerical upwind schemes to ensure global convergence of mass, momentum, energy and species. The turbulence model used was k-ε model, SST, SSG Reynolds with wall functions. The region of interest in the flow is divided into a grid. Each grid element is considered as a control volume with the properties constant over its volume.

"Analysis and Design of a Scramjet Engine Inlet Operating from Mach 5 to Mach 10" authored by Luu Hong Quan, Nguyen Phu Hung, Le Doan Quang, Vu Ngoc Long ref. ISSN: 2330-0248 (2016) gives a preliminary report of the analysis and design process of a scramjet engine inlet operating over a Mach number range from 5 to 10 without the use of variable geometry (moving parts) in order to find an optimal 2D geometry. An introduction of scramjet engine as well as its first component, the inlet, is given in the beginning and a number of basic inlet configurations are proposed. Inlet efficiency parameters and various design criteria are then explained, followed by a theoretical flow analysis utilizing some simplifying assumptions and the oblique shockwave relations. Parameters discussed in the paper were helpful for determination of a structured approach for our dissertation. Various Inlet parameters and geometries have been discussed in this paper.

"Hypersonic Intake Starting Characteristics–A CFD Validation Study" authored by Soumyajit Saha and Debasis Chakraborty ref. Defence Science Journal, Vol. 62, No. 3, May 2012, pp. 147-152, DOI: 10.14429/dsj.62.1340 (2012) provides numerical simulation of hypersonic intake starting characteristics. Three dimensional RANS equations are solved alongwith SST turbulence model using commercial computational fluid dynamics (CFD) software. Wall pressure distribution and intake performance parameters are found to match well with experimental data for different free stream Mach number in the range of 3-8. The governing equations used by the software have been highlighted in this paper. The analysis and the use of governing equations have been explained in brief.

III. MODELLING

The following figure shows a 2D cross-sectional sketch of the geometry considered. For analysis in ANSYS CFX, rather than modeling a solid geometry with an enclosure, just the model of the flow section was considered and the boundaries were considered as rigid walls. This was done as the primary concern was the propagation of the shocks and the quality of air throughout the section, rather than the effect on the model itself. Similarly, a 3D model was considered and analysis was done using ANSYS 16.0 CFX.

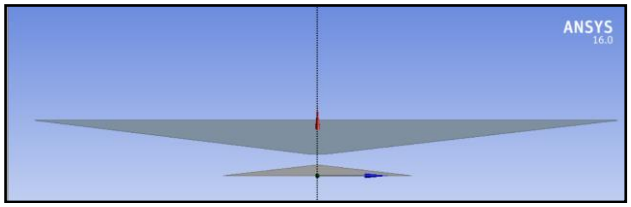

Fig. 2: 2D Sketch of Model

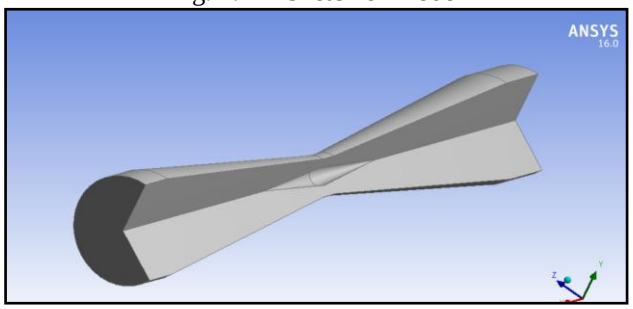

Fig. 3: 3D Representation of Flow Path

IV. MESHING

Meshing creation in is done with the help of required commands from the meshing creation tool pad. The meshing creation tool pad contains command buttons that allows performing operations which include creating edge meshing, face meshing and boundary conditions.

A mesh with suitable characteristics was created. The meshing was relatively finer at the juncture of oblique shock creation as well as in the throat section.

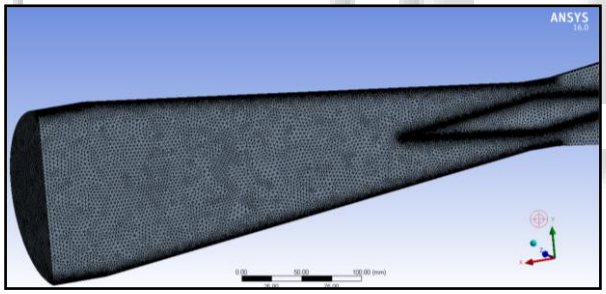

Fig. 4: Meshed Flow Path

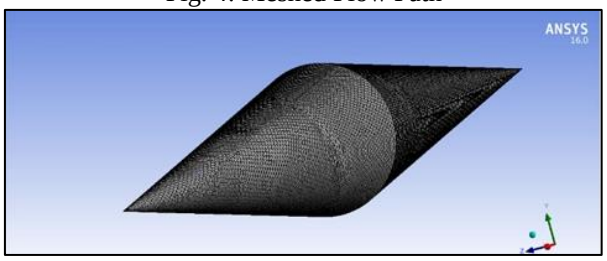

Fig. 5: Meshed Cowl Section

Statistics	
Nodes	671357
Elements	3523308
Mesh Metric	Element Quality
Min	0.21852
Max	1.
Average	0.83518
Standard Deviation	9.9113e-002

Table 1: Mesh Characteristics

Sizing	
Use Advanced Size F...	On: Curvature
Relevance Center	Fine
Initial Size Seed	Active Assembly
Smoothing	High
Transition	Slow
Span Angle Center	Fine
Curvature Normal ...	Default (18.0 °)
Min Size	Default (0.133650 mm)
Max Face Size	8.0 mm
Max Size	15.0 mm
Growth Rate	Default (1.20)
Minimum Edge Length	25.20 mm

Table 2: Sizing Characteristics

V. BOUNDARY CONDITIONS

A. *Turbulence Model*

K-epsilon (k-ε) turbulence model is used to simulate mean flow characteristics for turbulent flow conditions. It is a two equation model which gives a general description of turbulence by means of two transport equations which focus on 2 different variables

The first transported variable is the turbulence kinetic energy (k)

$$\frac{\partial}{\partial t}(\rho k)+\frac{\partial}{\partial x_i}(\rho k u_i)=\frac{\partial}{\partial x_j}\left[\left(\mu+\frac{\mu_t}{\sigma_k}\right)\frac{\partial k}{\partial x_j}\right]+P_k+P_b-\rho\epsilon-Y_M+S_k$$

The second transported variable is the rate of dissipation of turbulence energy (ε).

$$\frac{\partial}{\partial t}(\rho\epsilon)+\frac{\partial}{\partial x_i}(\rho\epsilon u_i)=\frac{\partial}{\partial x_j}\left[\left(\mu+\frac{\mu_t}{\sigma_\epsilon}\right)\frac{\partial \epsilon}{\partial x_j}\right]+C_{1\epsilon}\frac{\epsilon}{k}(P_k+C_{3\epsilon}P_b)-C_{2\epsilon}\rho\frac{\epsilon^2}{k}+S_\epsilon$$

The constants used are as follows

$C_\mu = 0.09$ $\sigma_k = 1.00$ $\sigma_\epsilon = 1.30$ $C_{1\epsilon} = 1.44$ $C_{2\epsilon} = 1.92$

This model was chosen for its computational versatility with minimal input requirements

B. *Sutherland Viscosity Law*

It gives relationship between dynamic viscosity, and the absolute temperature, of an ideal gas. It is based on kinetic theory of ideal gases and an idealized intermolecular-force potential. It is still commonly used and most often gives fairly accurate results with an error less than a few percent over a wide range of temperatures. Sutherland's law can be expressed as:

$$\mu = \mu_{ref}\left(\frac{T}{T_{ref}}\right)^{3/2}\frac{T_{ref}+S}{T+S}$$

T_{ref} is a reference temperature.

μ_{ref} is the viscosity at the T_{ref} reference temperature

S is the Sutherland temperature

Sutherland's law coefficients:

Gas	$\mu_0[\frac{kg}{ms}]$	$T_0[K]$	$S[K]$	$C_1[\frac{kg}{ms\sqrt{K}}]$
Air	1.716×10^{-5}	273.15	110.4	1.458×10^{-6}

Table 3:

Thus, realizing the nature of temperature variation in the flow, Sutherlands Law has been opted for

Gauge Pressure	2511.32 Pa
Mach Number	2.85
Reference Temperature	221.65 K
Turbulent Viscosity	0.01 Pa.s
Turbulent Ratio	10 %
Altitude	20 km

Table 4: Input Boundary Conditions

VI. PRE-OPTIMIZATION RESULTS

The results found by employing the above simulation methodology were found. They were then matched to available experimental data for validation. The experimental data was in the form of velocity values at a section 0.02m downstream of the throat section. Thus, data about the quality of air at that section was extracted from the simulation and compared with available experimental data. The table below gives the experimental values taken as reference for validation

MAXIMUM VELOCITY IN THROAT SECTION (AT x=0.02) (m/s)	FREESTREAM MACH NUMBER	MAXIMUM PRESSURE IN THROAT SECTION (AT x=0.02) (Pa)
800	2.8	1.115E+06
810	2.83	1.1158E+06
824.6	2.848	1.13E+06
840	2.87	1.135E+06
848	2.89	1.1832E+06
852	2.93	1.19E+06
860	2.96	1.1935E+06
865.2	2.975	1.192E+06
870	2.98	1.201E+06
878	3.01	1.209E+06

Table 5: Experimental Data

The velocity contour obtained was as follows. 2 cross sectional planes were inserted to highlight the throat section.

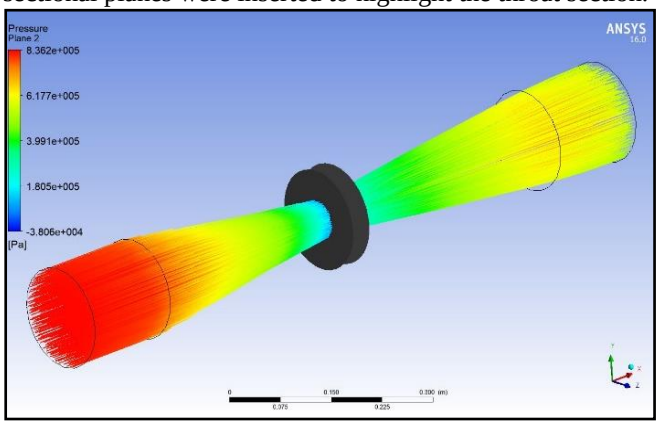

Fig. 6: Throat Velocity for Contour with Planes Highlighting Throat Section

Values of velocities at concerned sections in the geometry were found by putting probes at strategic places in CFX-Post module and by inserting CEL expressions and velocity values were obtained. The following images show values of velocity obtained for certain simulations

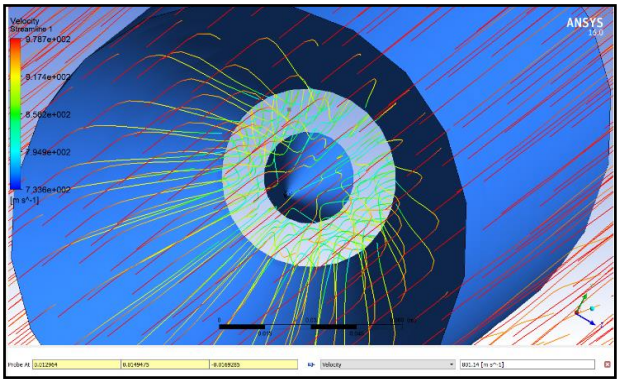

Fig. 7: Throat Velocity for Free Stream Mach number of 2.85

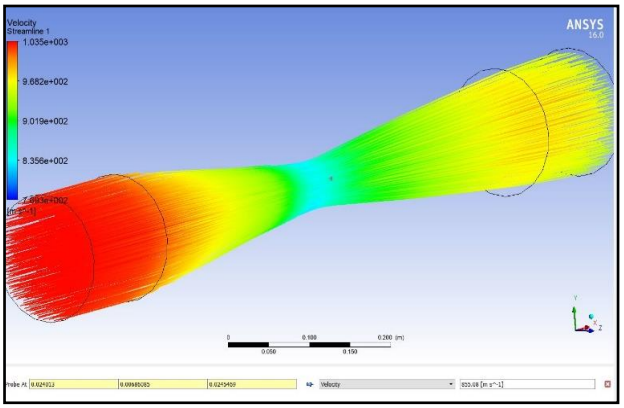

Fig. 8: Throat Velocity for Free Stream Mach number of 3.01

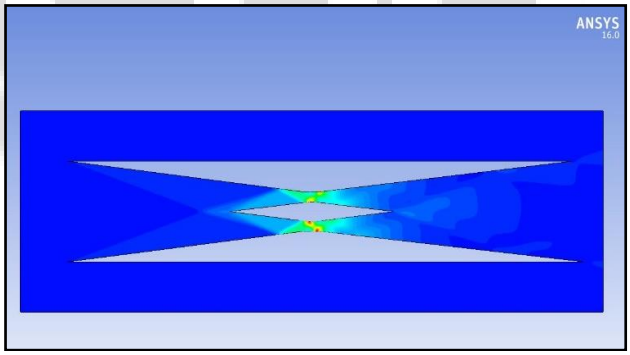

Fig. 9: Oblique Shock Propagation in 2D Cross-Sectional Model

Thus, the following table shows a comparative study of numerical and experimental results

Freestream Mach Number	Simulated value of velocity obtained at section 0.02 m downstream of throat (m/s)	Experimental value of velocity obtained at section 0.02 m downstream of throat (m/s)	Error Percentage (%)
2.85	801.59	824.6	2.79
3.01	855.08	878	2.61

Table 6: Simulation Results

As the above result table shows, velocity values are within an error percentage of 3% which is acceptable. Thus, it can be concluded that the methodology tested out is capable of providing highly accurate results to experimental

conditions and may be used to survey Mach domains beyond the range of available experimental data.

VII. POST OPTIMIZATION RESULTS

As per the results obtained by modeling of the flow section, the comparison of the same with experimental data yielded that optimization for inlet ramp angle and cowl tip angle would largely affect the outcome of velocity values. Thus, module for Response Surface Optimization was selected to be applied for calculating optimized angle values which result in lower starting Mach number. The value for velocity downstream of the throat section at y=0.02m was considered as the primary output by entering CEL expressions.

A. Design of Experiments (DOE)

Design of experiment (DOE) is a technique used to determine the location of sampling points and included as part of the Response Surface, Goal Driven Optimization and Six Sigma analysis systems. The Design of Experiment allows you to preview or generate and solve a DOE Design point matrix.

SR. No	Angle 1	Angle 2	Velocity
1	4.55	351	759.165
2	4.9995096388622189	350.00977645418607	733.188
3	4.9951800248236395	351.99067591852508	750.035
4	4.5499391344957987	350.00517497560941	751.35
5	4.5462688786792569	351.98840015684254	765.281
6	4.9977929595042951	351.00432592513971	742.802
7	4.3250116054783572	350.50509580713697	764.131
8	4.7725887312903073	350.49973932723515	746.809
9	4.7730019936920147	351.49172831024043	755.052
10	4.3286567518371157	351.48335616779514	770.527
11	4.32330031421734	351.99382065259852	774.738
12	4.774719457386527	350.99637287273072	750.931
13	4.5493249331484549	350.49988581356592	755.299
14	4.77038583616959	351.98460371582769	757.266
15	4.7784821674809788	350.00493698357604	742.217
16	4.9993264056392945	350.49997374298982	736.355
17	4.9969120495603416	351.50090351956896	744.688
18	4.549559434491675	351.50063600740395	763.849
19	4.3192221090779634	350.99683205061592	768.846
20	4.328994297783356	350.01854658056982	760.824

Table 7: List of multiple design points in DOE

The Max and Min values of velocity as per custom sampling method narrowed down the range as per figure below.

Properties of Outline A9: P4 - VelocityVal

	A	B
1	Property	Value
2	General	
3	Component ID	Response Surface
4	Directory Name	RSO
5	Units	m s^-1
6	Notes	
7	Notes	
8	Values	
9	Calculated Minimum	733.19
10	Calculated Maximum	780.78
11	Output Settings	
12	Transformation Type	Yeo-Johnson

Fig. 9: Max and Min Values of Output Throat Section Velocity Response Surface

ANSYS Design Xplorer includes industry-leading algorithms, as well as many industry standard algorithms, that analyzed the table of design points to produce a response surface. One can use the response surface to instantly predict the performance of the design without needing to run the actual simulation. This reduced order meta-model can then be used for sensitivity studies, optimization and six sigma analysis.

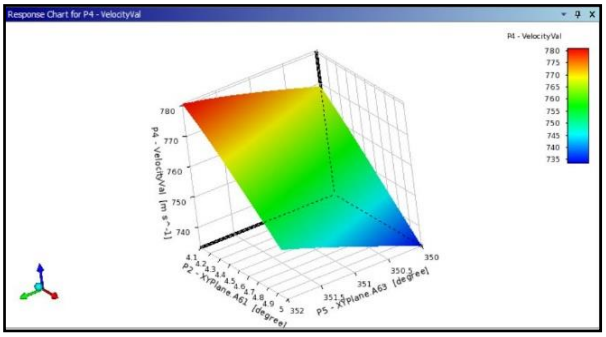

Fig. 10: Overall 3D Response Chart for Both Angular Inputs

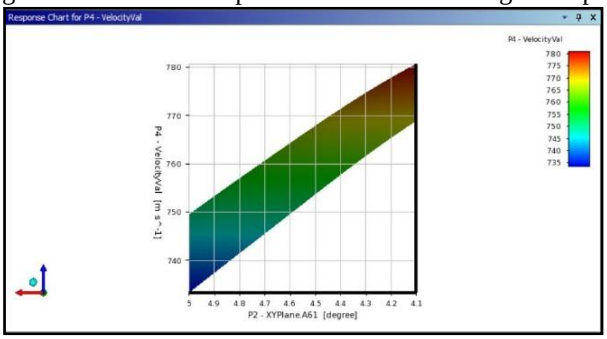

Fig. 11: Wedge Angle to Velocity Relation Response Chart

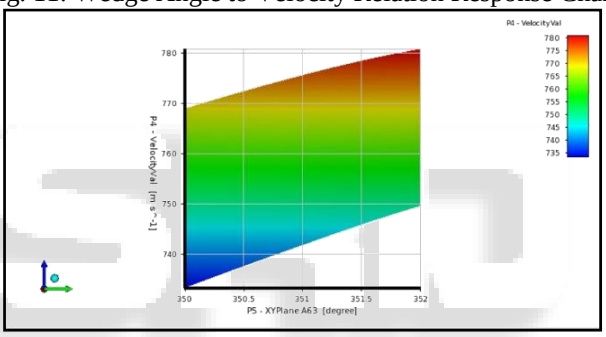

Fig. 12: Cowl Section Angle to Velocity Relation Response Chart

Response surface module also maps other important characteristics which determine accurate converged results in form of candidate points and respective tradeoffs between points.

Table of Schematic B4: Optimization | Candidate Points

	A	B	C	D	E	F
1	Reference	Name	P2 - XYPlane.A61 (degree)	P5 - XYPlane.A63 (degree)	P4 - VelocityVal (m s^-1)	
2					Parameter Value	Variation from Reference
3	◉	Candidate Point 1	4.1	352	780.78	0.00%
4	○	Candidate Point 2	4.1068	351.75	779.5	-0.16%
5	○	Candidate Point 3	4.1032	351.5	778.36	-0.31%
*		New Custom Candidate Point	4.55	351		

(a): Candidate Points

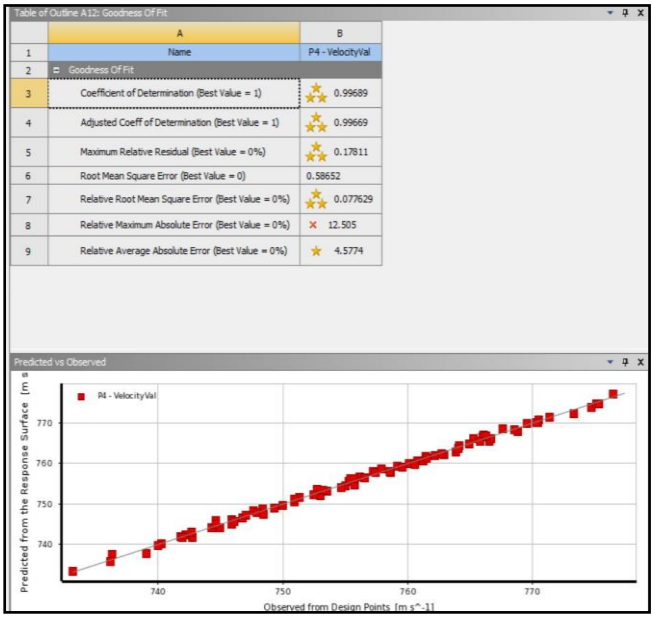

(b): Goodness of Fit

B. Optimization

Algorithms in this module can search the design space with direct solvers or use the response surface. One can take multiple objectives, constraints and parameter relationships into account, easily define them in the user interface. Design Xplorer tracks the progress of the optimization and produces a variety of charts and tables that make it possible to evaluate trade-offs and choose from the best design candidates.

Optimization Study			
Maximize P4	Goal, Maximize P4 (Default importance)		
Optimization Method			
Screening	The Screening optimization method uses a simple approach based on sampling and sorting. It supports multiple objectives and constraints as well as all types of input parameters. Usually it is used for preliminary design, which may lead you to apply other methods for more refined optimization results.		
Configuration	Generate 1000 samples and find 3 candidates.		
Status	Converged after 1000 evaluations.		
Candidate Points			
	Candidate Point 1	Candidate Point 2	Candidate Point 3
P2 - XYPlane.A61 (degree)	4.1	4.1068	4.1032
P5 - XYPlane.A63 (degree)	352	351.75	351.5
P4 - VelocityVal (m s^-1)	780.78	779.5	778.36

Fig. 11: Optimized Angles with Respective Velocity

Thus the above table gives inlet geometry parameters viz. the inlet wedge angles for which suitable velocities may be obtained.

Wedge Angle in degrees	Cowl Angle in degrees	Velocity in (m/s)
4.1	8	780.78
4.1068	8.25	779.5
4.1032	8.5	778.36

Table 7:

VIII. CONCLUSION

Thus, the optimization results show that Mach reduction achieved is considerable and should provide conditions in the combustion chamber suitable for successful starting and thrust production. It also needs to be noted that the complexity of the problem may be further increased by monitoring pressure and temperature variation. This would require a lot of resources. However, it is clearly established that, should they be available, this area warrants further research.

